

Hydrogen Production *via* Acetic Acid Steam Reforming over HZSM-5 and Pd/HZSM-5 Catalysts and Subsequent Mechanism Studies

Qi Wang,^a Shurong Wang,^{b,*} Xinbao Li,^b and Long Guo^b

Acetic acid (HOAc) was selected as a bio-oil model compound for the steam reforming of bio-oil for hydrogen production. The influence of temperature and steam-to-carbon ratio (S/C) on the steam reforming of HOAc over hydrogen-type Zeolite Socony Mobil-5 (HZSM-5) and the catalyst with added Pd (Pd/HZSM-5) have been investigated in a fixed-bed reactor. Brunauer–Emmett–Teller surface area measurements, scanning electron microscopy, and transmission electron microscopy were performed to characterize the texture and structure of the catalysts. Upon addition of Pd to HZSM-5, the selectivity of the products was modified and the H₂ yield was greatly increased. The hydrogen yield and potential hydrogen yield from the steam reforming of HOAc were as high as 60.2% and 87.5%, respectively, under optimized reaction conditions. Both the conversion of HOAc and the H₂ yield over Pd/HZSM-5 were significantly enhanced with increasing S/C ratio and reaction temperature below 600 °C, whereas the H₂ yield did not significantly increase at temperatures above 600 °C. The mechanism of HOAc decomposition on the Pd(111) surface was calculated *via* density functional theory. The optimal decomposition route was found to be CH₃COOH* → CH₃CO* → CH₃* + CO*.

Keywords: Bio-oil; Steam reforming; Hydrogen; Zeolite; Acetic acid; Density functional theory

Contact information: a: College of Metrological Technology and Engineering, China Jiliang University, Hangzhou 310018, PR China; b: State Key Laboratory of Clean Energy Utilization, Zhejiang University, Hangzhou 310027, PR China; *Corresponding author: srwang@zju.edu.cn

INTRODUCTION

As a promising resource for clean energy, hydrogen offers great potential for utilization in fuel cells, which may provide power for automobiles in the future (Chalk and Miller 2006). Currently, the most widely used methods for hydrogen production are steam reforming of natural gas and naphtha, as well as gasification of coal followed by shift conversion (Ahn and Fischer 1986). These processes, however, produce great quantities of greenhouse gases. In contrast, biomass is carbon-neutral because the carbon released during the biomass utilization process is reabsorbed by growing plants. Therefore, ever-increasing interest has been recently directed toward hydrogen production from environmentally friendly biomass (Davda *et al.* 2005).

Developments in fast pyrolysis technologies in the last few decades have facilitated bio-oil production from biomass at high yield and efficiency. Bio-oil is a complex mixture of water and oxygenated organic compounds, the latter of which include alcohols, carboxylic acids, aldehydes, sugars, phenolics, and ketones. Compared with other fuels produced from biomass, bio-oil has the advantage of higher energy density and high transportability. However, its large-scale utilization has been limited by

its disadvantages such as high oxygen content, high water content, low calorific value, high viscosity, and corrosiveness. Several methods used in upgrading other fuels have been introduced into the bio-oil upgrading process, such as catalytic cracking, catalytic hydrogenation, esterification, gasification for synthesis gas (syngas), and steam reforming for hydrogen production.

Bio-oil catalytic steam reforming for hydrogen production is an economically feasible way of producing hydrogen. As an integrated process, it can markedly reduce the cost of hydrogen production from bio-oil and thus allow it to be competitive with the well-developed process of hydrogen production by steam reforming of natural gas (Czernik *et al.* 2002, 2007). In bio-oil catalytic steam reforming, the aqueous fraction of bio-oil is used to produce hydrogen, while the lignin-derived fraction is utilized for the production of phenolic resins and other chemicals. Domine *et al.* (2008) used Pt- and Rh-based catalysts for the steam reforming of bio-oil and consistently obtained H₂ yields as high as 70% at a steam-to-carbon ratio (S/C) of 10 and temperature (*T*) of 780 °C. Rennard *et al.* (2010) investigated the performance of Rh–Ce catalysts in the production of syngas by partial oxidation and steam reforming of bio-oil. They reported that Rh catalysts achieved high conversion to H₂ and CO, and that the process could either be achieved autothermally or with additional heat for higher H₂ yield.

However, due to the complexity of bio-oil, model compounds are required to establish the catalyst structure–activity correlations. Acetic acid (HOAc), one of the major components of bio-oil, can reach concentrations as high as 32 wt % (Wang *et al.* 1996; Takanabe *et al.* 2004, 2006). Considerable effort has been devoted to the catalytic steam reforming of HOAc. Takanabe *et al.* (2006) carried out the catalytic steam reforming of HOAc over the noble-metal-based catalyst Pt/ZrO₂ and obtained 100% HOAc conversion and 87% H₂ yield at 875 K and S/C = 5. Bimbela *et al.* (2007) prepared three different Ni–Al coprecipitated catalysts and systematically studied the influence of various factors on the performance of the HOAc steam reforming reaction. These factors are the catalyst reduction time, the reaction temperature, the catalyst weight/HOAc flow-rate ratio, and the nickel content of the catalyst. Somsak *et al.* (2001) compared the effects of various metal oxide supports (Al₂O₃, Ce_{1-x}–Zr_xO₂, and MgO) on the performance of HOAc catalytic steam reforming over Ni-supported catalysts. Their results show that the Ni/Ce_{0.75}Zr_{0.25}O₂ catalyst exhibited superior activity with 98.84% HOAc conversion and 99.34% H₂ yield.

Zeolites are multiporous crystalline solids with well-organized porous structures, and are widely used as catalysts in heterogeneous catalysis. Their high surface area and surface acidity can facilitate a variety of catalytic reactions. The hydrogen-type Zeolite Socony Mobil-5 (HZSM-5) has also been used as a support in the catalytic cracking of hydrocarbons and in a dimethyl ether reforming process. Its high efficiency in the dehydrogenation and rupture of C–C bonds has been reported by many researchers (Kawabata *et al.* 2006; Semelsberger *et al.* 2006). However, to our knowledge, there are few reports on bio-oil steam reforming over zeolites, in particular, HZSM-5. Furthermore, information on the mechanism of HOAc decomposition on the transition-metal surface is still limited.

In the present study, hydrogen production from HOAc over HZSM-5 catalysts with a Pd content of 5 wt% (5% Pd/HZSM-5) was investigated. Moreover, density functional theory (DFT) calculations for HOAc decomposition on the Pd surface were carried out. The study aimed at evaluating the performance of HZSM-5 in the production of hydrogen by bio-oil reforming and the effect of adding Pd to HZSM-5 on the catalytic

performance. For this purpose, the features of the Pd/HZSM-5 catalyst were investigated by various characterization methods, and the influence of reaction parameters (T and S/C) on the catalytic performance was explored in detail.

EXPERIMENTAL AND COMPUTATIONAL METHODS

Catalyst Preparation

Samples of 5% Pd/HZSM-5 were prepared by the incipient wetness impregnation method, using $\text{Pd}(\text{NO}_3)_2$ as a precursor. The HZSM-5 was calcined in air at 500 °C for 2 h before impregnation. A measured amount of $\text{Pd}(\text{NO}_3)_2$ was dissolved in a quantity of a HNO_3 solution in deionized water. To this mixture was added the HZSM-5 powder at a liquid/solid ratio of 1.5 mL/g. The resulting slurry was stirred vigorously and then dried under an infrared lamp until the water was completely removed. The dried sample was calcined at 500 °C for 3 h, and then crushed and sieved to 40–60 mesh.

Characterization of the Catalysts

The texture and structure of the freshly made catalysts were measured by the N_2 adsorption–desorption method, using a Tristar 3000 physisorption analyzer (Micromeritics, USA).

Images of both fresh and spent HZSM-5 and 5% Pd/HZSM-5 were acquired by scanning electron microscopy (SEM) using an FEI Model SiRION-100 scanning electron microscope.

Images for transmission electron microscopy (TEM) were obtained using a Philips Tecnai G2F30.

Catalyst Testing

The catalysts were tested in a continuous, fixed-bed reactor. The experimental system is shown in Fig. 1. The heating rate and the furnace temperature were controlled by an electric furnace. The reaction temperature, which was controlled within the range of 400 to 750 °C, was monitored by a thermocouple placed at the center of the catalyst layer. The catalyst (1 mL) was diluted with 2 mL of quartz sand and packed in a quartz tube reactor with an inner diameter of 8 mm. Prior to the reaction, the catalyst was reduced with H_2 at 400 °C for 3 h. A thermocouple was placed in the center of the reactor to monitor its real temperature. The feedstock was fed into the reactor by means of a syringe pump. Prior to the inlet of the reactor, the premixed reactants were vaporized to ensure their thorough distribution throughout the catalyst bed. Nitrogen was used as carrier gas and was introduced at a flow rate of 30 mL/min. The $G_{\text{C}_1\text{HSV}}$ (carbon equivalent space velocity) was kept at 345 h^{-1} . The S/C ratio was maintained within the range of 2.5 to 9.2 by adjusting the concentration of HOAc aqueous solution in the feedstock. The products were condensed in the condenser system. The uncondensed gases were dried and analyzed with an online gas chromatograph. Levels of H_2 , N_2 , CO , and CO_2 in the gases were measured by means of a thermal conductivity detector, while those of CH_4 and C_2 – C_3 gases were measured by means of a hydrogen flame ionization detector.

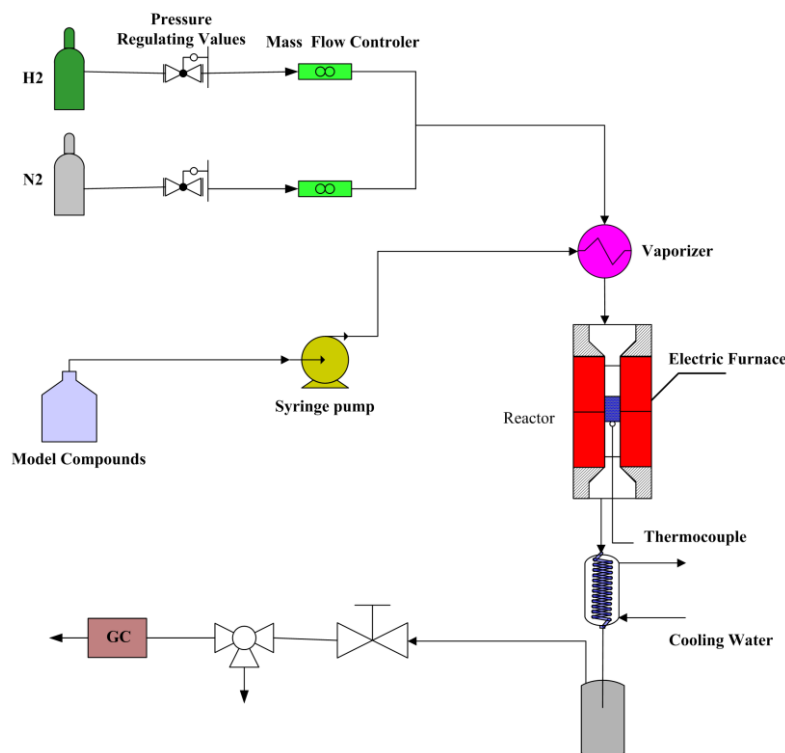


Fig. 1. Schematic diagram of the experimental system

HOAc steam reforming was carried out at various values of T and S/C ratios. The hydrogen yield (Eq. (1)) was defined as a percentage of the stoichiometric H₂ potential. The HOAc conversion (Eq. (2)) was calculated as the number of moles of carbon in the gaseous products divided by the number of moles of carbon in the feed (all carbons were from HOAc). The carbon selectivity (Eq. (3)) was calculated as the number of moles of carbon in each respective gaseous product (CO, CO₂, CH₄, and C₂–C₃) divided by the number of moles of carbon converted.

$$\text{H}_2 \text{ yield \%} = \frac{\text{moles of H}_2 \text{ obtained}}{\text{stoichiometric H}_2 \text{ potential}} \times 100\% \quad (1)$$

$$\text{HOAc Conversion \%} = \frac{\text{moles of carbon (in CO + CO}_2 + \text{CH}_4 + \text{C}_{2-3}) \text{ obtained}}{\text{moles of carbon in the feed}} \times 100\% \quad (2)$$

$$\text{Carbon Selectivity \%} = \frac{\text{moles of carbon in one gas product}}{\text{moles of carbon converted}} \times 100\% \quad (3)$$

Computational Method

The total energy calculations using the spin-polarized periodic DFT approach were performed *via* the Vienna Abinitio simulation package (VASP). The exchange–correlation functional was calculated within the generalized gradient approximation (GGA) proposed by Perdew, Burke, and Ernzerhof (PBE). Ionic cores were described by the projector-augmented wave (PAW) pseudopotential, and the cutoff energy was set at 400 eV. The Pd(111) slab models, which consisted of three metal layers, were construc-

ted based on a 3×2 unit cell. The Brillouin zone was sampled with a $6 \times 6 \times 1$ Monkhorst–Pack k-point mesh. The Fermi smearing was set to 0.1 eV. The transition state (TS) and the energy barrier were determined by the nudged elastic band (NEB) method (Mills *et al.* 1995). A series of images along the path of the reactants and the products of each elementary reaction were generated by linear interpolation and then optimized by the NEB algorithm. The TS was identified as the image with the highest energy. A set of 10 images that contained the initial state (IS) and the final state (FS) were used in the NEB calculations. The energy barrier of each elementary reaction was calculated from the energy difference between the TS and IS. All atoms were relaxed, and the energy and force were converged to 10^{-4} eV and 0.05 eV/Å, respectively.

RESULTS AND DISCUSSION

Catalyst Characterization

Brunauer–Emmett–Teller surface area (S_{BET})

Table 1 contains the textural properties of the Pd/HZSM-5 and HZSM-5 catalysts. The addition of Pd led to a decrease in the S_{BET} , pore volume, and average pore diameter. The S_{BET} of HZSM-5 and Pd/HZSM-5 were 365.1 and 333.7 m^2/g , respectively.

Table 1. Brunauer–Emmett–Teller (BET) Surface Area, Pore Volume, and Pore Diameter of the Fresh Catalysts

Sample	S_{BET} (m^2/g)	V_P (cm^3/g)	V_M (cm^3/g)	D_P (nm)
HZSM-5	365.1	0.081	0.119	7.18
5% Pd/HZSM-5	333.7	0.048	0.109	4.24

S_{BET} : BET surface area, V_P : cumulative pore volume calculated from the Barrett–Joyner–Halenda (BJH) desorption isotherm; V_M : micropore volume calculated by the t-plot method; D_P : BJH desorption average pore diameter

The N_2 adsorption–desorption isotherms for Pd/HZSM-5 and HZSM-5 are shown in Fig. 2.

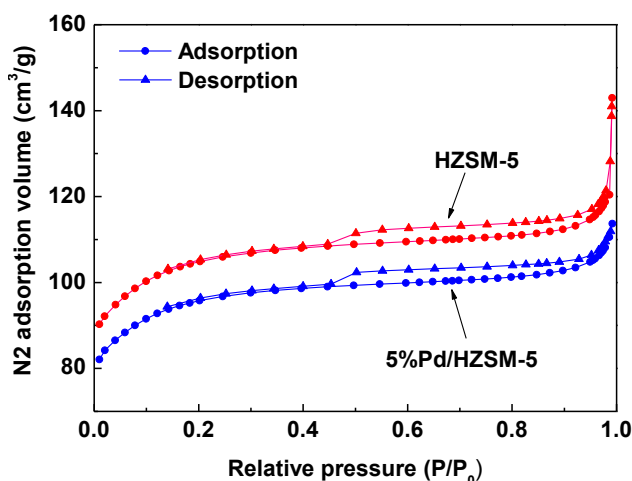


Fig. 2. N_2 adsorption–desorption isotherms of the prepared catalysts

Both of the prepared catalysts exhibited a type IV isotherm (International Union of Pure and Applied Chemistry classification of adsorption isotherm features), which indicates a mesoporous structure. Both of the catalyst samples presented H4-type hysteresis over a wide range of P/P_0 values, indicating that the mesopores were slitlike structures formed from the interparticle voids created by the arrangement of zeolite crystallites.

SEM and TEM

SEM images of the freshly made and spent catalyst were acquired to ascertain the possible influence of palladium on the carbon deposits. Figure 3 shows the surface morphologies of (a) fresh Pd/HZSM-5, (b) spent Pd/HZSM-5, (c) fresh HZSM-5, and (d) spent HZSM-5. Both of the fresh catalysts had a stacked-particle structure and high crystallinity. It is interesting to note that carbon filaments were generated after the steam reforming of HOAc on the Pd/HZSM-5 and HZSM-5 catalysts. The carbon filaments could be lengthened on the Pd/HZSM-5 catalyst. The generation of carbon filaments here may be attributed to the catalytic decomposition of hydrocarbons (C_2H_4 and C_2H_6) produced in the steam reforming process of HOAc.

TEM images of the fresh, bare HZSM-5 and Pd/HZSM-5 (Fig. 4) show that Pd was highly dispersed in the HZSM-5 support, and its particle size was around 10 nm.

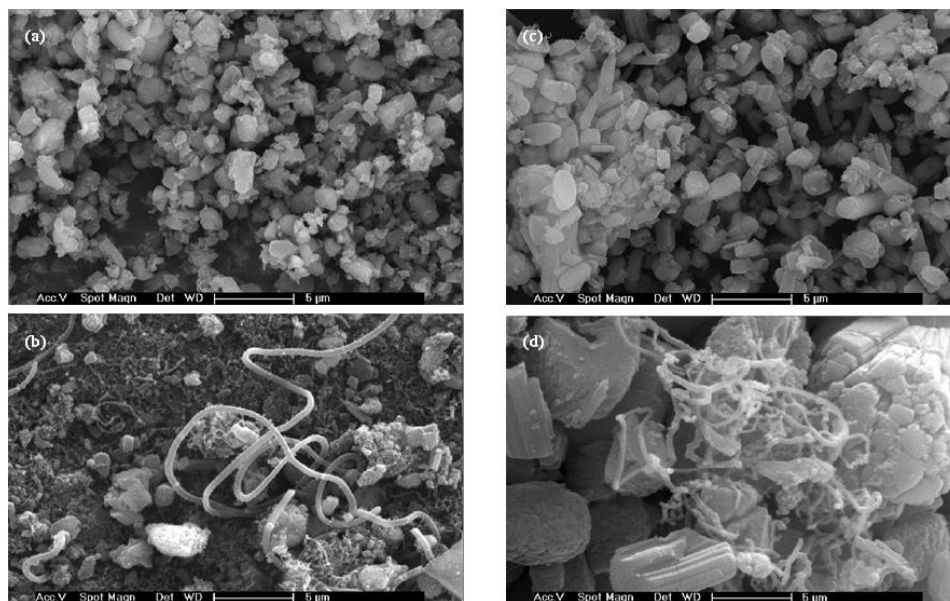


Fig. 3. SEM images of fresh catalysts and spent catalysts in the catalytic steam reforming of acetic acid at 600 °C, S/C = 9.2. (a) Fresh Pd/HZSM-5, (b) spent Pd/HZSM-5, (c) fresh HZSM-5, and (d) spent HZSM-5

Catalytic Performance

Influence of reaction temperature

Figures 5 and 6 show the results on the performance of catalytic steam reforming of HOAc at various temperatures over HZSM-5 and Pd/HZSM-5 catalysts, respectively. The H_2 yields over HZSM-5 were much lower than those over Pd/HZSM-5 at all reaction temperatures. It is also worth noting that at lower temperatures (400 and 500 °C) over the HZSM-5 catalyst (Fig. 5), the HOAc conversion remained low, but when the temperature was increased to 600 °C, there was a marked increase in conversion (74.9%).

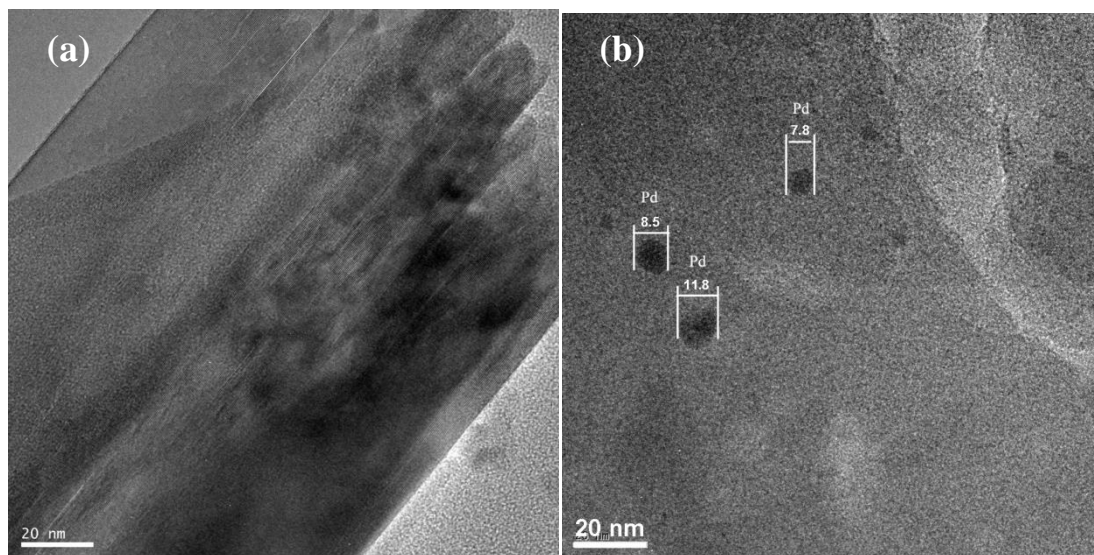


Fig. 4. TEM image of fresh Pd/HZSM-5 catalyst. (a) HZSM-5 and (b) Pd/HZSM-5

These changes accompanied the increased selectivities of CO and light hydrocarbons (C_2H_4 , C_2H_6 , and C_3H_8), which were products of the thermal decomposition of HOAc. C_2H_4 showed the highest selectivity among hydrocarbons at 600 °C, whereas the selectivity of C_3H_8 reached 19.4% at 750 °C. In contrast, the CO_2 selectivity over the bare HZSM-5 catalyst decreased significantly with the temperature increase. This decrease suggests that the water gas shift (WGS) reaction ($CO + H_2O \rightarrow CO_2 + H_2$) was inhibited with increasing temperature, especially above 600 °C. At relatively low temperature (400 °C), the WGS reaction was preferred over thermal decomposition, so that the main carbon-containing product was CO_2 . Thus, increasing temperature inhibited the WGS reaction and led to decomposition of more HOAc to CO and hydrocarbons over HZSM-5. These resulted in the decrease in CO_2 selectivity and the increase in selectivities of CO and light hydrocarbons. The high selectivity of light hydrocarbons could promote chemical vapor decomposition, and thus lead to the generation of carbon filaments as well.

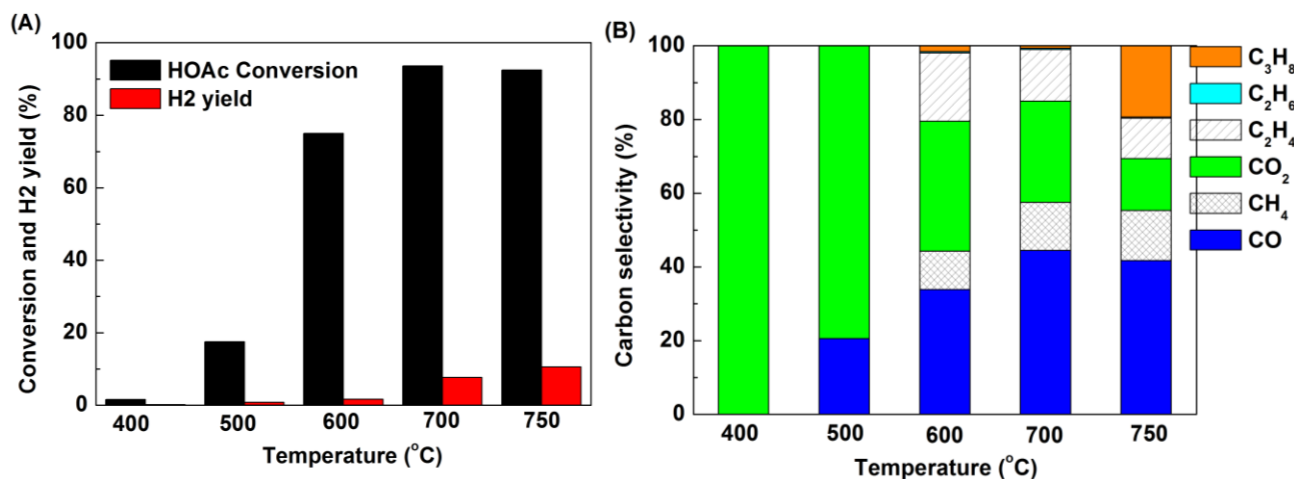


Fig. 5. Steam reforming of acetic acid over HZSM-5 catalyst at different temperatures: (A) hydrogen yield and carbon conversion, and (B) selectivity of carbon-containing gases. Reaction conditions: S/C = 9.2, $G_{C_1HSV} = 345 \text{ h}^{-1}$

Figure 6A shows the results on the hydrogen yield and HOAc conversion over Pd/HZSM-5. An increase in reaction temperature generally led to a significantly increased hydrogen yield and HOAc conversion, especially in the range of 400 to 600 °C. This tendency is consistent with results obtained over other catalysts (Li *et al.* 2011; Yan *et al.* 2010). The H₂ yield and HOAc conversion over Pd/HZSM-5 at 400 °C were 5.7% and 32.9%, respectively, and increased at 600 °C to 60.2% and 95.7%, respectively. The HOAc conversion was similar to the results obtained by Somsak *et al.* (2011), whereas the H₂ yield was less than their reported values (the HOAc conversion and H₂ yield reached 98.84% and 99.34%, respectively, over 15% Ni/Ce_{0.75}Zr_{0.25}O₂). As shown in Fig. 6B, the selectivity for C₂H₄ reached 38.2% at 400 °C. On increasing the temperature from 400 °C to 750 °C, the C₂H₄ selectivity decreased markedly to 0.5%. In addition, the selectivity of CO and CO₂ increased with increasing temperature. Above 600 °C, CO and CO₂ became the major gaseous products, whereas CH₄ and other hydrocarbons were present in trace amounts. Therefore, the Pd/HZSM-5 catalyst suppressed the conversion of HOAc to CH₄ at all tested temperatures. A comparison of the HOAc conversion and the H₂ yield over the two catalysts clearly showed that both could be significantly increased by addition of Pd to HZSM-5. Below 600 °C, the selectivity of CO₂ was much lower on the Pd/HZSM-5 catalyst compared with the selectivity on the HZSM-5 catalyst. This difference indicates that formation of CO and light hydrocarbons from the decomposition of HOAc was enhanced by the addition Pd at low temperature. The WGS reaction was also enhanced, leading to the increase in H₂ yield. Additionally, high selectivities of C₃H₈ were obtained at temperatures lower than 700 °C for Pd/HZSM-5 and as high as 750 °C for HZSM-5. The difference in temperature can be ascribed to the enhancement of steam reforming reactions by the addition of Pd (carbon precursors such as C_xH_y compounds react with OH formed by decomposition of H₂O to form CO). Although the formation of C₃H₈ via HOAc decomposition over HZSM-5 increased with temperature, the depletion of C₃H₈ and the concomitant formation of CO due to steam reforming over Pd/HZSM-5 at high temperature sharply increased. The same trend was observed with C₂H₆, C₂H₄, and CH₄. As a result, the CO and CO₂ selectivities over the Pd/HZSM-5 catalyst increased with increasing temperature, whereas those of the light hydrocarbons (C₃H₈, C₂H₆, C₂H₄, and CH₄) decreased.

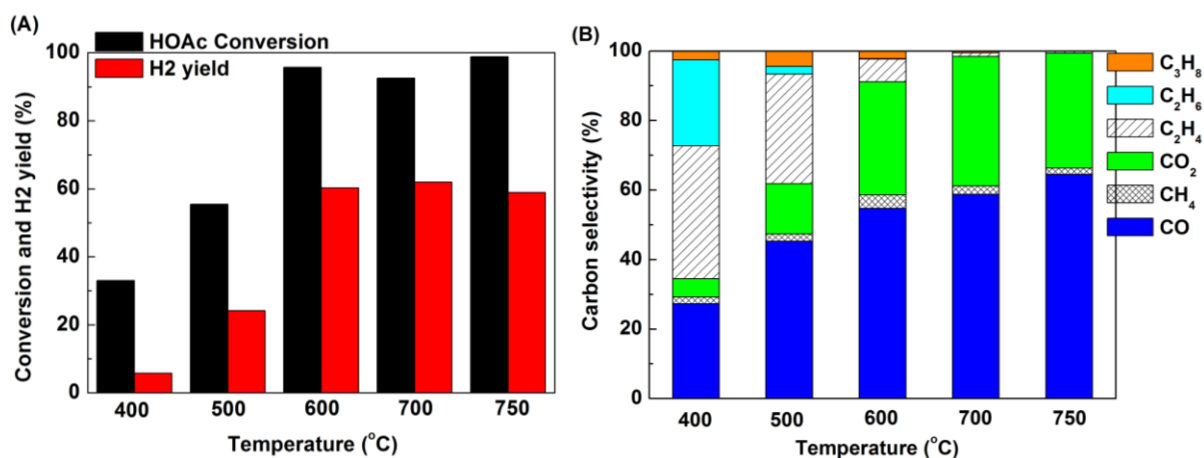


Fig. 6. Steam reforming of acetic acid over Pd/HZSM-5 catalyst at different temperatures: (A) hydrogen yield and carbon conversion and (B) selectivity of carbon-containing gases. Reaction conditions: S/C = 9.2, G_{C1}HSV = 345 h⁻¹

Influence of S/C ratio

Besides the temperature, the S/C ratio is another important factor that affects catalytic activity. In our study, the S/C ratio is defined as follows:

$$S/C = \frac{\text{moles of gas water in the feed}}{\text{moles of carbon in the feed}} \times 100\% \quad (4)$$

Figure 7 shows the influence of S/C on the conversion, H₂ yield, and selectivity of carbon-containing gases (CO, CO₂, CH₄, C₂H₄, C₂H₆, and C₃H₈) of HOAc steam reforming over Pd/HZSM-5 catalyst at $T = 600\text{ }^{\circ}\text{C}$ and $G_{C1}HSV = 345\text{ h}^{-1}$. Figure 7A clearly shows that both the carbon conversion and H₂ yield were enhanced with increasing S/C ratio. The H₂ yield and carbon conversion at S/C = 2.5 were 24.5% and 30.1%, respectively, and increased to 60.2% and 95.7%, respectively, at S/C = 9.2.

As shown in Fig. 7B, the selectivity for CO decreased, while that for CO₂ increased when the S/C ratio increased from 2.5 to 9.2. The addition of steam allowed steam reforming and the WGS reaction to prevail. Carbon monoxide is one of the major byproducts of the bio-oil steam reforming process. HOAc steam reforming over Pd/HZSM-5 showed high CO selectivity.

Considering that the CO generated in the reforming process could be readily used to generate H₂ through the additional WGS reaction at relatively low temperature, the potential H₂ yield can be described as follows:

$$\text{Potential H}_2 \text{ yield \%} = \frac{\text{moles of H}_2 \text{ and CO obtained}}{\text{stoichiometric H}_2 \text{ potential}} \times 100\% \quad (5)$$

The potential H₂ yield of the steam reforming of HOAc at $T = 600\text{ }^{\circ}\text{C}$, $S/C = 9.2$, and $G_{C1}HSV = 345\text{ h}^{-1}$ was 87.5%, which was markedly higher than the hydrogen yield in Fig. 7A. Therefore, the process combining bio-oil steam reforming with WGS reaction in a two-stage reactor has great potential for production of high-purity hydrogen.

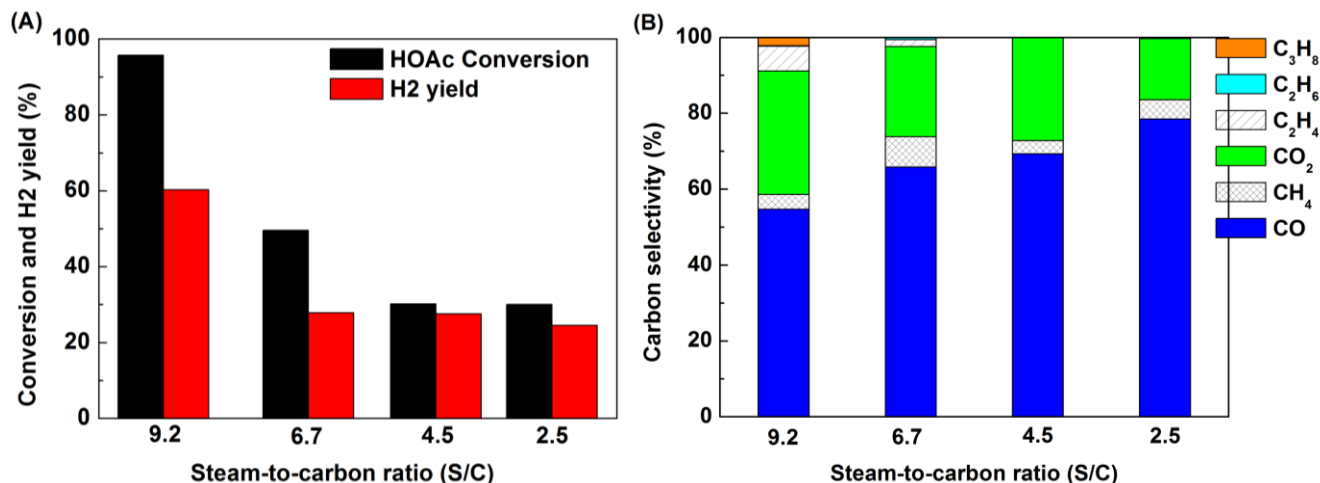


Fig. 7. Steam reforming of acetic acid over Pd/HZSM-5 catalyst at various S/C ratios: (A) hydrogen yield and carbon conversion and (B) selectivity of carbon-containing gases. Reaction conditions: $T = 600\text{ }^{\circ}\text{C}$, $G_{C1}HSV = 345\text{ h}^{-1}$

HOAc Decomposition Mechanism

According to our TEM measurement, the Pd particle size in HZSM-5 was about 10 nm, which provided a sufficiently large Pd surface for HOAc decomposition. The Pd(111) surface has been widely chosen as a model system for studying the decomposition of oxygenated organic, such as ethanol and methanol (Jiang *et al.* 2009; Gu and Li 2010; Li *et al.* 2010). Therefore, we carried out a study on the HOAc decomposition mechanism on the Pd(111) surface.

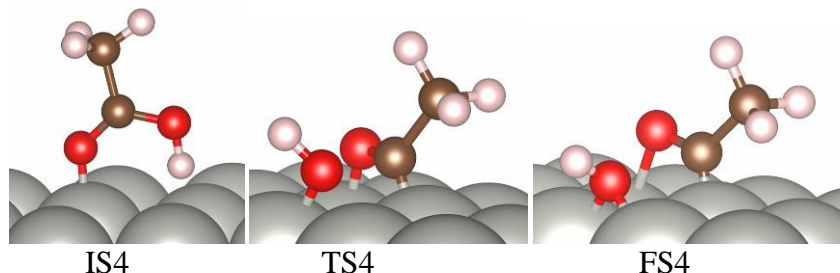
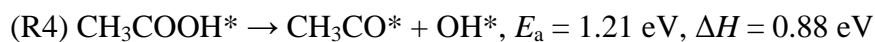
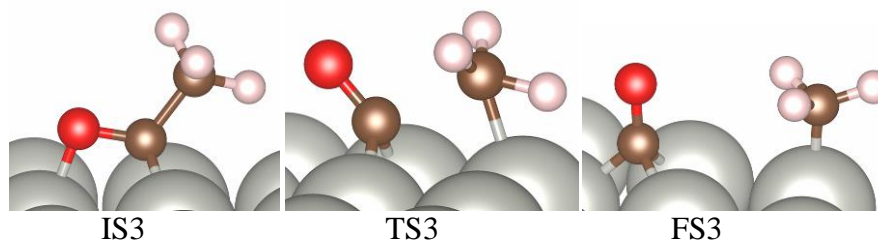
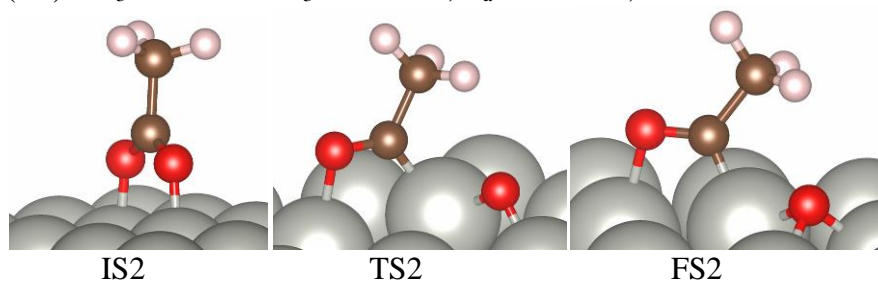
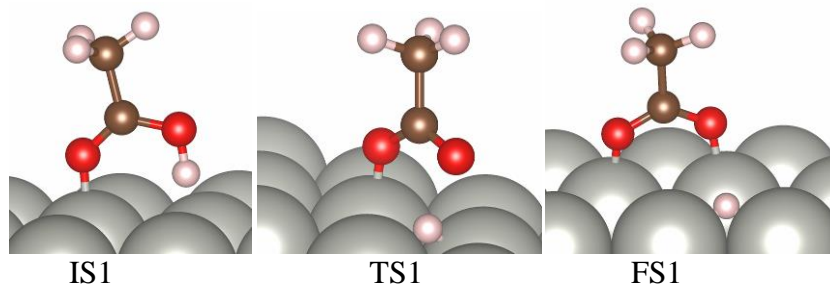
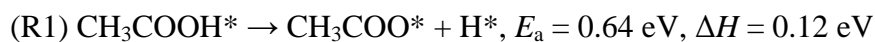


Fig. 8. Energy barriers and geometries of acetic acid decomposition on the Pd(111) surface

The possible reaction energy barriers and each IS, TS, and FS geometries of the HOAc decomposition elementary reactions are shown in Fig. 8. Results from our previous studies (Wang *et al.* 2012) suggest that there are two possible routes for the decomposition. One route is initiated by dehydrogenation (the asterisk represents the surface site): $\text{CH}_3\text{COOH}^* \rightarrow \text{CH}_3\text{COO}^* \rightarrow \text{CH}_3\text{CO}^* \rightarrow \text{CH}_3^* + \text{CO}^*$. The other route is initiated by dehydroxylation: $\text{CH}_3\text{COOH}^* \rightarrow \text{CH}_3\text{CO}^* \rightarrow \text{CH}_3^* + \text{CO}^*$. As shown in Fig. 8, the rate-determining step in the former route is R2, with an energy barrier of 1.85 eV. In contrast, the rate-determining step in the latter possible route is R4, with an energy barrier of 1.21 eV, which is much lower than R2. Therefore, the optimal HOAc decomposition route on the Pd(111) surface is $\text{CH}_3\text{COOH}^* \rightarrow \text{CH}_3\text{CO}^* \rightarrow \text{CH}_3^* + \text{CO}^*$.

CONCLUSIONS

1. Pd/HZSM-5 catalyst containing 5 wt% Pd was prepared by an incipient wet impregnation method. Pd/HZSM-5 and HZSM-5 were characterized in detail by N_2 adsorption measurements, SEM and TEM.
2. HOAc could be converted efficiently on the bare HZSM-5 catalyst at high temperature (600 to 750 °C), but the corresponding H_2 yields were all lower than 11%.
3. With Pd/HZSM-5, the H_2 yield was significantly increased and the product distribution was modified. The H_2 yield and potential H_2 yield for HOAc steam reforming over Pd/HZSM-5 were as high as 60.2% and 87.5% at $T = 600$ °C, $S/C = 9.2$, and $G_{\text{C}_1\text{HSV}} = 345 \text{ h}^{-1}$.
4. The optimal HOAc decomposition route on the Pd(111) surface is $\text{CH}_3\text{COOH}^* \rightarrow \text{CH}_3\text{CO}^* \rightarrow \text{CH}_3^* + \text{CO}^*$. The rate-determining step is $\text{CH}_3\text{COOH}^* \rightarrow \text{CH}_3\text{CO}^* + \text{OH}^*$, which has an energy barrier of 1.21 eV.

ACKNOWLEDGMENTS

The authors are grateful for the financial support from the National Science Foundation for Young Scholars of China (51106145), the Program for Zhejiang Leading Team of S&T Innovation (2009R50012), and the Key Laboratory of Renewable Energy and Gas Hydrate, Chinese Academy of Sciences (Y007K9).

REFERENCES CITED

- Ahn, Y. K., and Fischer, W. H. (1986). "Production of hydrogen from coal and petroleum coke: Technical and economic perspectives," *Int. J. Hydrogen Energ.* 11(12), 783-788.
- Bimbela, F., Oliva, M., Ruiz, J., García, L., and Arauzo, J. (2007). "Hydrogen production by catalytic steam reforming of acetic acid, a model compound of biomass pyrolysis liquids," *J. Anal. Appl. Pyrolysis.* 79(1-2), 112-120.

- Chalk, S. G., and Miller, J. F. (2006). "Key challenges and recent progress in batteries, fuel cells, and hydrogen storage for clean energy systems," *J. Power Sources* 159(1), 73-80.
- Czernik, S., French, R., Feik, C., and Chornet, E. (2002). "Hydrogen by catalytic steam reforming of Liquid byproducts from biomass thermoconversion Processes," *Ind. Eng. Chem. Res.* 41(17), 4209-4215.
- Czernik, S., Evans, R., and French, R. (2007). "Hydrogen from biomass-production by steam reforming of biomass pyrolysis oil," *Catal. Today* 129(3-4), 265-268.
- Davda, R. R., Shabaker, J. W., Huber, G. W., Cortright, R. D., and Dumesic, J. A. (2005). "A review of catalytic issues and process conditions for renewable hydrogen and alkanes by aqueous-phase reforming of oxygenated hydrocarbons over supported metal catalysts," *Appl. Catal. B - Environ.* 56(1-2), 171-186.
- Domine, M. E., Iojoiu, E. E., Davidian, T., Guilhaume, N., and Mirodatos, C. (2008). "Hydrogen production from biomass-derived oil over monolithic Pt- and Rh-based catalysts using steam reforming and sequential cracking processes," *Catal. Today* 133-135, 565-573.
- Gu, X., and Li, W. (2010). "First-principles study on the origin of the different selectivities for methanol steam reforming on Cu(111) and Pd(111)," *J. Phys. Chem. C*, 114, 21539-21547.
- Jiang, R., Guo, W., Li, M., Fu, D., and Shan, H. (2009). "Density functional investigation of methanol dehydrogenation on Pd(111)," *J. Phys. Chem. C*, 113, 4188-4197.
- Kawabata, T., Matsuoka, H., and Shishido, T. (2006). "Steam reforming of dimethyl ether over ZSM-5 coupled with Cu/ZnO/Al₂O₃ catalyst prepared by homogeneous precipitation," *Appl. Catal. A - General* 308(10), 82-90.
- Li, M., Guo, W., Jiang, R., Zhao, L., and Shan, H., (2010). "Decomposition of ethanol on Pd(111): A density functional theory study," *Langmuir* 26 (3), 1879-88.
- Li, X., Wang, S., Cai, Q. (2011). "Effects of preparation method on the performance of Ni/Al₂O₃ catalysts for hydrogen production by bio-oil steam reforming," *Appl. Biochem. Biotech.* 168(1), 10-20.
- Mills, G., Jonsson, H., and Schenter, G. K. (1995). "Reversible work transition state theory: Application to dissociative adsorption of hydrogen," *Surf. Sci.* 324, 305-337.
- Rennard, D., French, R., Czernik, S., Josephson, T., and Schmidt, L. (2010). "Production of synthesis gas by partial oxidation and steam reforming of biomass pyrolysis oils," *Int. J. Hydrogen Energ.* 35(9), 4048-4059.
- Semelsberger, T. A., Ott, K. C., and Borup, R. L. (2006). "Generating hydrogen-rich fuel-cell feeds from dimethyl ether (DME) using physical mixtures of a commercial Cu/Zn/Al₂O₃ catalyst and several solid-acid catalysts," *Appl. Catal. B - Environ.* 65(3-4), 291-300.
- Takanabe, K., Aika, K. I., Seshan, K., and Lefferts, L. (2004). "Sustainable hydrogen from bio-oil: steam reforming of acetic acid as a model oxygenate," *J. Catal.* 227(1), 101-108.
- Takanabe, K., Aika, K. I., Seshan, K., and Lefferts, L. (2006). "Catalyst deactivation during steam reforming of acetic acid over Pt/ZrO₂," *Chem. Eng. J.* 120(1-2), 133-137.
- Wang, D., Montané, D., and Chornet, E. (1996). "Catalytic steam reforming of biomass-derived oxygenates: Acetic acid and hydroxyacetaldehyde," *Appl. Catal. A - General* 143, 245-270.

- Wang, S., Li, X., Guo, L., and Luo, Z., (2012). "Experimental research on acetic acid steam reforming over Co-Fe catalysts and subsequent density functional theory studies," *Int. J. Hydrogen Energ.* 37(15), 11122-11131.
- Yan, C., Cheng, F., and Hu, R. (2010). "Hydrogen production from catalytic steam reforming of bio-oil aqueous fraction over Ni/CeO₂-ZrO₂ catalysts," *Int. J. Hydrogen Energ.* 35(21), 11693-11699.

Article submitted: January 31, 2013; Peer review completed: March 3, 2013; Revised version received and accepted: April 22, 2013; Published: April 26, 2013.